Advances in Applied Mathematics and Mechanics
Adv. Appl. Math. Mech., Vol. 7, No. 4, pp. 454-471

DOI: 10.4208/aamm.2013.m401
August 2015

Optimal Bicubic Finite Volume Methods on Quadrilateral Meshes

Yanli Chen[1] and Yonghai Li[2,*]

[1] *Institute of Mathematics, Jilin University, Changchun 130012, China*
[2] *School of Mathematics, Jilin University, Changchun 130012, China*

Received 11 November 2013; Accepted (in revised version) 27 October 2014

Abstract. In this paper, an optimal bicubic finite volume method is established and analyzed for elliptic equations on quadrilateral meshes. Base on the so-called element-wise stiffness matrix analysis technique, we proceed the stability analysis. It is proved that the new scheme has optimal $\mathcal{O}(h^3)$ convergence rate in H^1 norm. Additionally, we apply this analysis technique to bilinear finite volume method. Finally, numerical examples are provided to confirm the theoretical analysis of bicubic finite volume method.

AMS subject classifications: 65N30, 65N15

Key words: Finite volume method, bicubic element, quadrilateral meshes.

1 Introduction

Finite volume methods (FVMs) [1–14, 16], also known as generalized difference methods [17–24], box schemes [25–27], covolume methods [28], have been one class of the most commonly used numerical methods for solving partial differential equations in practice. Generally speaking, FVMs are flexible to handle complicated domain geometries and boundary conditions. More important, FVMs can preserve the local conservation of certain physical quantities (e.g., mass, momentum, and energy), so they have enjoyed great popularity in many fields, such as computational fluid dynamics, computational aerodynamics, petroleum engineering and so on.

The FVMs for elliptic equations on triangulation have been much studied in the literature [3, 5, 8, 13, 17, 18, 25, 26, 29, 35]. On the other hand, the FVMs on quadrilateral meshes are also commonly used in the physical applications. Many early results have been published on the accuracy of FVM with isoparametric bilinear finite element on

*Corresponding author.
Email: chenyanli7532@sina.com (Y. L. Chen), yonghai@jlu.edu.cn (Y. H. Li).

 ©2015 Global Science Press

https://doi.org/10.4208/aamm.2013.m401 Published online by Cambridge University Press

quadrilateral meshes. The authors of [21] and [27] studied H^1 error estimate and obtained $\|u-u_h\|_1 \leq Ch|u|_2$ independently. In 2007, Yang [10] constructed a second-order finite volume method on quadrilateral meshes. In comparison to Yang [10], Lv [12] established an optimal biquadratic finite volume method on quadrilateral meshes which has optimal $\mathcal{O}(h^2)$ convergence rate in H^1 norm and $\mathcal{O}(h^3)$ convergence rate in L^2 norm. In this paper, we constructed and analyzed an optimal bicubic finite volume method, which is a natural next step in setting up a theoretical basis.

It was known that the stability analysis is a difficult task in error estimates for higher order FVMs. The traditional analysis method is the so-called element stiffness matrix analysis, in which all eigenvalues of an element stiffness matrix often need to be calculated. In order to keep the ellipticity of the bilinear form of FVMs, the minimum eigenvalue of an element stiffness matrix needs to be positive, which requires the mesh to satisfy certain geometric requirements (cf. e.g., [10, 12, 14, 19–21, 35]). Zhang and Zou [31] provide a unified analysis for FVMs of any order on rectangular meshes, in which the stability analysis technique surpasses the so-called elementwise stiffness matrix technique. By a special mapping, the proof of stability avoids calculating eigenvalues of an element stiffness matrix and the global inf-sup condition is established for FVMs of any order.

The remainder of the present paper is organized as follows. In Section 2, we introduce some necessary notations and assumptions, and construct the bicubic finite volume method. Section 3 is devoted to H^1 error estimate. In Section 4, we apply the so-called elementwise stiffness matrix analysis technique to the stability analysis of bilinear finite volume element method. In the last section, numerical examples are presented to confirm the theoretical analysis of bicubic finite volume method.

2 Bicubic finite volume method

In this section we propose the bicubic finite volume method on quadrilateral meshes to solve the following elliptic boundary value problem

$$-\nabla\cdot(A(x,y)\nabla u) = f \qquad \text{in } \Omega, \tag{2.1a}$$

$$u = 0 \qquad \text{on } \partial\Omega, \tag{2.1b}$$

where $\Omega \subset \mathbb{R}^2$ is a bounded convex polygon with boundary $\partial\Omega$, and $f \in L^2(\Omega)$. The coefficient $A(x,y) = (a_{ij}(x,y))_{i,j=1}^2$, whose entries $a_{ij} \in C^1(\Omega)$, is assumed to be symmetric, bounded and uniformly positive definite in $\overline{\Omega}$; i.e., there exist two positive constants C_1 and C_2 such that

$$C_1\boldsymbol{\xi}^T\boldsymbol{\xi} \leq \boldsymbol{\xi}^T A(x,y)\boldsymbol{\xi} \leq C_2\boldsymbol{\xi}^T\boldsymbol{\xi}, \quad \forall \boldsymbol{\xi} \in \mathbb{R}^2, \quad \forall (x,y) \in \overline{\Omega}. \tag{2.2}$$

Divide $\overline{\Omega}$ into a sum of finite number of strictly convex quadrilaterals such that different quadrilaterals have no common interior point, that a vertex of any quadrilateral does not lie on the interior of a side of any other quadrilateral, and that any vertex of

https://doi.org/10.4208/aamm.2013.m401 Published online by Cambridge University Press

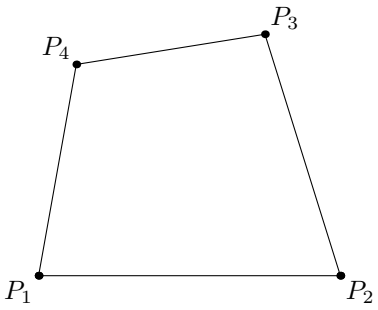


Figure 1: Quadrilateral element.

the boundary is a vertex of some quadrilateral. Then we obtained a primal partition $\mathcal{T}_h$, where h is the largest diameter of all quadrilaterals.

Let h_K denote the diameter of the element $K\in\mathcal{T}_h$, ρ_K denote the maximum diameter of circles contained in K, and S_K denote the area of K.

Suppose $\mathcal{T}_h$ is regular, i.e., there exist positive constants C and C_1 such that for any element $K\in\mathcal{T}_h$

$$\frac{h_K}{\rho_K}\leq C, \tag{2.3a}$$

$$|\cos\theta_K|\leq C_1, \quad \text{where } \theta_K \text{ is any interior angle of } K. \tag{2.3b}$$

Following the terminology from [29], a quadrilateral K is called an $h^{1+\tau}$-parallelogram if it satisfies

$$|\overrightarrow{P_1P_2}+\overrightarrow{P_3P_4}|\leq Ch^{1+\tau}, \tag{2.4}$$

where $0<\tau\leq 1$ and P_i, $i=1,2,3,4$, are the vertices of the quadrilateral K as in Fig. 1. An $h^{1+\tau}$-parallelogram is also called "almost a parallelogram". This assumption on quadrilateral is commonly used in the FVMs [9,12,16,21,27] and the FEMs [29,32].

We take the unit square $\widehat{K}=[0,1]\times[0,1]$ as the reference element in the $\xi\eta$-plane with vertices denoted by

$$\widehat{P}_1=(0,0), \quad \widehat{P}_2=(1,0), \quad \widehat{P}_3=(1,1), \quad \widehat{P}_4=(0,1).$$

Let K be a convex quadrilateral with the $P_i=(x_i,y_i)$ $(i=1,2,3,4)$ of the vertices placed counterclockwise as in Fig. 1. Then there exists a unique invertible bilinear transformation F_K which maps $\widehat{K}$ onto K and satisfies

$$P_i=F_K(\widehat{P}_i), \quad i=1,2,3,4.$$

In fact, it is given by

$$\begin{cases} x=x_1+a_1\xi+a_2\eta+a_3\xi\eta, \\ y=y_1+b_1\xi+b_2\eta+b_3\xi\eta, \end{cases} \tag{2.5}$$

https://doi.org/10.4208/aamm.2013.m401 Published online by Cambridge University Press

where

$$a_1=x_2-x_1, \quad a_2=x_4-x_1, \quad a_3=x_1-x_2+x_3-x_4,$$
$$b_1=y_2-y_1, \quad b_2=y_4-y_1, \quad b_3=y_1-y_2+y_3-y_4.$$

Denote the Jacobian matrix of F_K by $\mathcal{J}_K$, and the determinant of $\mathcal{J}_K$ by J_K, then

$$\mathcal{J}_K=\begin{pmatrix}\frac{\partial x}{\partial\xi} & \frac{\partial x}{\partial\eta}\\ \frac{\partial y}{\partial\xi} & \frac{\partial y}{\partial\eta}\end{pmatrix}=\begin{pmatrix}a_1+a_3\eta & a_2+a_3\xi\\ b_1+b_3\eta & b_2+b_3\xi\end{pmatrix}.$$

Simple calculation shows that J_K is a linear function of ξ and η:

$$J_K(\xi,\eta)=\alpha_K+\beta_K\xi+\gamma_K\eta,$$

where

$$\alpha_K=2S_{\triangle P_1P_2P_3}, \quad \beta_K=2(S_{\triangle P_1P_2P_3}-S_{\triangle P_1P_2P_4}), \quad \gamma_K=2(S_{\triangle P_1P_3P_4}-S_{\triangle P_1P_2P_4}),$$

and $S_{\triangle P_iP_jP_k}$ denote the area of the triangular $\triangle P_iP_jP_k$. For any $M\subset\mathbb{R}^2$, we define $|g(x,y)|_{\infty,M}:=\sup_{(x,y)\in M}|g(x,y)|$. If quadrilateral element K is an $h^{1+\tau}$-parallelogram, then

$$|J_K|_{\infty,\widehat{K}}\le Ch_K^2, \quad |J_K^{-1}|_{\infty,K}\le Ch_K^{-2}.$$

On the reference element $\widehat{K}$, we select 16 notes $\widehat{P}_{k,l}=(\sigma_k,\sigma_l)$, for $k,l=1,2,3,4$, with

$$\sigma_1=0, \quad \sigma_2=\frac{1}{2}-\frac{\sqrt{5}}{10}, \quad \sigma_3=\frac{1}{2}+\frac{\sqrt{5}}{10}, \quad \sigma_4=1.$$

We let $\widehat{Q}_{i,j}=(e_i,e_j)$, for $i,j=0,1,2,3,4$, with

$$e_0=0, \quad e_1=\frac{1}{2}-\frac{\sqrt{15}}{10}, \quad e_2=\frac{1}{2}, \quad e_3=\frac{1}{2}+\frac{\sqrt{15}}{10}, \quad e_4=1.$$

For each element $K\in\mathcal{T}_h$, let $P_{k,l}=F_K(\widehat{P}_{k,l})$ and $Q_{i,j}=F_K(\widehat{Q}_{i,j})$, as in Fig. 2. We define the control volumes in K of the nodes $P_{k,l}$ by the subregions $Q_{k-1,l-1}Q_{k,l-1}Q_{k,l}Q_{k-1,l}$, where $Q_{0,0}=P_{1,1}$, $Q_{4,0}=P_{4,1}$, $Q_{4,4}=P_{4,4}$, and $Q_{0,4}=P_{1,4}$. For each node P, denote the associate control volume by K_P^*. Then if P is the inner vertex, K_P^* is the union of the above subregions, sharing the vertex P. If P is the node on one edge of some element, K_P^* is the union of the above subregions, sharing the common edge including P. If P is the inner nodes of some element K, K_P^* the above subregion, being part of K. The set of all the control volumes forms a dual partition $\mathcal{T}_h^*$.

https://doi.org/10.4208/aamm.2013.m401 Published online by Cambridge University Press

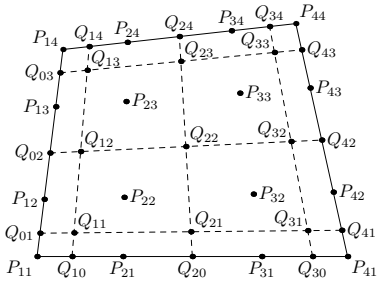


Figure 2: Control volumes in a quadrilateral element for bicubic element.

The trial function space U_h is chosen as a finite element space associated with the primal partition $\mathcal{T}_h$. Denote by $U_h(\widehat{K})$ the standard bicubic polynomial space on $\widehat{K}$, then defined the trial function space as

$$U_h=\{u_h\in H_0^1(\Omega):u_h|_K=\widehat{u}_h\circ F_K^{-1},\ \widehat{u}_h\in U_h(\widehat{K}),\ K\in\mathcal{T}_h\}.$$

Define the test function space as

$$V_h=\{v_h\in L^2(\Omega):v_h|_{K_P^*}=\text{constant},\ P\in\dot{\Omega}_h\},$$

where $\dot{\Omega}_h$ denote the set of all the interpolation nodes. Let Π_h be the usual nodal interpolation operator from $U=H_0^1(\Omega)\cap H^4(\Omega)$ onto U_h, Π_h^* be the interpolation operator from U_h onto the test function space V_h, then (cf. [33])

$$|u-\Pi_h u|_m\le Ch^{4-m}\|u\|_4,\quad m=0,1,2,3,\quad \forall u\in U, \tag{2.6a}$$
$$|w_h-\Pi_h^* w_h|_0\le Ch|w_h|_1,\quad w_h\in U_h. \tag{2.6b}$$

The finite volume element methods for (2.1a) and (2.1b) is to find $u_h\in U_h$ such that

$$a(u_h,v_h)=(f,v_h),\quad v_h\in V_h, \tag{2.7}$$

with

$$a(u_h,v_h)=-\sum_{K_P^*}\int_{\partial K_P^*}(A\nabla u_h)\cdot\mathbf{n}v_h ds,\quad (f,v_h)=\sum_{K_P^*}\int_{K_P^*}fv_h dxdy,$$

where $P\in\dot{\Omega}$ and $\mathbf{n}$ is the outward unit normal vector of ∂K_P^*.

3 H^1 error estimate

Before proceeding to the error analysis of the finite volume method, we introduce the following discrete semi-norm $|\cdot|_{1,h}$ for U_h

$$|u_h|_{1,h}=\Big(\sum_{K\in\mathcal{T}_h}|u_h|_{1,h,K}^2\Big)^{\frac{1}{2}},\quad \forall u_h\in U_h, \tag{3.1}$$

https://doi.org/10.4208/aamm.2013.m401 Published online by Cambridge University Press

where

$$|u_h|^2_{1,h,K}=\sum_{l=1}^{4}\sum_{k=1}^{3}\big(u_h(P_{k+1,l})-u_h(P_{k,l})\big)^2+\sum_{k=1}^{4}\sum_{l=1}^{3}\big(u_h(P_{k,l+1})-u_h(P_{k,l})\big)^2.$$

The following lemma gives the equivalence between the above discrete semi-norm and the associate continuous semi-norm.

Lemma 3.1. *The norms $|\cdot|_{1,h}$ and $|\cdot|_1$ are equivalent in U_h, i.e., there exist positive constants C_1, C_2 independent of U_h such that*

$$C_1|u_h|_{1,h}\le|u_h|_1\le C_2|u_h|_{1,h},\quad \forall u_h\in U_h. \tag{3.2}$$

Proof. One can proceed similarly as Lemma 3.5 in [10] to complete the proof of this lemma. □

We now investigate the ellipticity of the bilinear form $a(\cdot,\Pi_h^*\cdot)$, which is crucial for the error analysis of the finite volume method. The proof of it relies on the following lemma about partitioned matrix.

Lemma 3.2. *Let $\mathcal{A}$ and $\mathcal{B}$ be two $n\times n$ matrices. The constant $\kappa\neq 0$. Then the matrix*

$$\begin{pmatrix}\mathcal{A} & \kappa\mathcal{B}\\ \kappa\mathcal{B}^T & \kappa^2\mathcal{A}\end{pmatrix}$$

is positive definite if and only if the matrices

$$\mathcal{A}\pm\frac{\mathcal{B}^T+\mathcal{B}}{2}$$

are positive definite.

Proof. The proof can be found in [10]. □

Following the technique from [12], for each $K\in\mathcal{T}_h$ with the average center Q, we denote

$$\bar{A}_K=\begin{pmatrix}a_{22}(Q) & -a_{12}(Q)\\ -a_{21}(Q) & a_{11}(Q)\end{pmatrix}.$$

Noting that $\bar{A}_K$ is a real symmetry matrix, it has the factorization

$$\bar{A}_K=Q_K^T\Lambda_K Q_K,$$

where Λ_K is a diagonal matrix whose diagonal entries are the eigenvalues of $\bar{A}_K$, and Q_K is an orthogonal matrix. Due to the ellipticity condition (2.2), Λ_K is positive definite. We now define an invertible mapping $\mathcal{F}_{K_A}$ by for $\mathbf{x}=(x,y)\in K$,

$$\mathcal{F}_{K_A}(\mathbf{x}):=Q_K^T\Lambda_K^{1/2}Q_K\mathbf{x},$$

https://doi.org/10.4208/aamm.2013.m401 Published online by Cambridge University Press

and let $K_A := \mathcal{F}_{K_A}(K)$ and vector $\widetilde{P_iP_j} := \mathcal{F}_{K_A}(\overrightarrow{P_iP_j})$, where $\overrightarrow{P_iP_j}$ is an edge of the element K. We define

$$\widetilde{\mathcal{T}_h} := \{K_A : K_A = \mathcal{F}_{K_A}(K),\ \forall K \in \mathcal{T}_h\}.$$

The introduce of the mapping $\mathcal{F}_{K_A}$ is a key skill to deal with variable matrix coefficient A. If A is an identity matrix, this maping changes nothing obviously. The element K_A is formed by coupling the quadrilateral K with the coefficient A indeed. Hereinafter, we would rather consider K_A only than dispose of the element K and the matrix A simultaneously.

The following regularity assumption in [12] on the partition $\mathcal{T}_h$ and the coefficient $A(x,y)$ will be used in our analysis.

Regularity assumption KA. All the inner angles of all the elements in $\widetilde{\mathcal{T}_h}$ are uniformly bounded away from zero and π, and the ratios between the length of the smallest edge and the longest edge of any element K_A are uniformly bounded away from zero.

Lemma 3.3. *Suppose that the partition $\mathcal{T}_h$ satisfies the condition* (2.4) *and Regularity assumption KA. Then for sufficiently small h, there exists a positive constant C such that*

$$a(u_h, \Pi_h^* u_h) \geq C\|u_h\|_1^2, \quad u_h \in U_h. \tag{3.3}$$

Proof. Rearranging the terms by element gives

$$\begin{aligned} a(u_h, \Pi_h^* u_h) &= -\sum_{K_P^* \in \mathcal{T}_h^*} \int_{\partial K_P^*} (A\nabla u_h)\cdot \mathbf{n} \Pi_h^* u_h ds \\ &:= \sum_{K\in\mathcal{T}_h} I_K(u_h, \Pi_h^* u_h), \quad \forall u_h \in U_h, \end{aligned} \tag{3.4}$$

with

$$\begin{aligned} I_K(u_h, \Pi_h^* \bar{u}_h) = &\sum_{k=1}^{3}\sum_{l=1}^{4} (\bar{u}_h(P_{k+1,l}) - \bar{u}_h(P_{k,l})) \int_{\overline{Q_{k,l}Q_{k,l-1}}} (A\nabla u_h)\cdot \mathbf{n} ds \\ &+ \sum_{l=1}^{3}\sum_{k=1}^{4} (\bar{u}_h(P_{k,l+1}) - \bar{u}_h(P_{k,l})) \int_{\overline{Q_{k,l}Q_{k-1,l}}} (A\nabla u_h)\cdot \mathbf{n} ds, \end{aligned} \tag{3.5}$$

where $K \in \mathcal{T}_h$, as shown as Fig. 2. Define an approximate bilinear form $\tilde{I}_K(\cdot,\cdot)$ on K as follows:

$$\begin{aligned} \tilde{I}_K(u_h, \Pi_h^* \bar{u}_h) = &\sum_{k=1}^{3}\sum_{l=1}^{4} (\bar{u}_h(P_{k+1,l}) - \bar{u}_h(P_{k,l})) \int_{\overline{Q_{k,l}Q_{k,l-1}}} (A(Q)\nabla u_h)\cdot \mathbf{n} ds \\ &+ \sum_{l=1}^{3}\sum_{k=1}^{4} (\bar{u}_h(P_{k,l+1}) - \bar{u}_h(P_{k,l})) \int_{\overline{Q_{k,l}Q_{k-1,l}}} (A(Q)\nabla u_h)\cdot \mathbf{n} ds, \end{aligned}$$

where Q is the average center of the element K.

https://doi.org/10.4208/aamm.2013.m401 Published online by Cambridge University Press

Let $X_{u_h,K}$ and $Y_{u_h,K}$ denote two row vectors related to u_h on K (as in Fig. 2) satisfying

$$X_{u_h,K}\equiv\big(u_h(P_{k+1,l})-u_h(P_{k,l})\big)_{j=1}^{12},\quad Y_{u_h,K}\equiv\big(u_h(P_{l,k+1})-u_h(P_{l,k})\big)_{j=1}^{12},$$

where $k=[(j-1)/4]+1$, $l=(j-1)(\mathrm{mod}4)+1$, and set $\alpha=(X_{u_h,K},Y_{u_h,K})$. Denote by

$$\phi_1(t)=-\frac{1}{\sigma_2\sigma_3}(t-\sigma_2)(t-\sigma_3)(t-1),\qquad \phi_2(t)=\frac{1}{\sigma_2(\sigma_2-\sigma_3)(\sigma_2-1)}t(t-\sigma_3)(t-1),$$
$$\phi_3(t)=\frac{1}{\sigma_3(\sigma_3-\sigma_2)(\sigma_3-1)}t(t-\sigma_2)(t-1),\quad \phi_4(t)=\frac{1}{(1-\sigma_2)(1-\sigma_3)}t(t-\sigma_2)(t-\sigma_3),$$

the cubic basis in one dimension, then

$$\tilde{I}_K(u_h,\Pi_h^*u_h)=\alpha\mathcal{A}\alpha^T=\alpha\frac{\mathcal{A}+\mathcal{A}^T}{2}\alpha^T,\tag{3.6}$$

where the block matrix

$$\mathcal{A}=\begin{pmatrix}\mathcal{A}_1 & \mathcal{A}_2\\ \mathcal{A}_3 & \mathcal{A}_4\end{pmatrix}.$$

To specify the entries of these matrices, let

$$\zeta_j(t)=\begin{cases}-\phi_1'(t), & j=1,\\ -\phi_1'(t)-\phi_2'(t), & j=2,\\ \phi_4'(t), & j=3,\end{cases}$$

and

$$A_1(\xi)=\left(\int_{\hat{I}_i}\frac{\phi_j(\eta)}{J_K(\xi,\eta)}\mathrm{d}\eta\right)_{i,j=1}^{4},\qquad A_4(\eta)=\left(\int_{\hat{I}_i}\frac{\phi_j(\xi)}{J_K(\xi,\eta)}\mathrm{d}\xi\right)_{i,j=1}^{4},$$
$$A_2^l(\xi)=\left(\phi_j(\xi)\int_{\hat{I}_i}\frac{-\zeta_l(\eta)(1-\eta)}{J_K(\xi,\eta)}\mathrm{d}\eta\right)_{i,j=1}^{4},\quad l=1,2,3,\qquad \bar{A}_2^l(\xi)=\left(\phi_j(\xi)\int_{\hat{I}_i}\frac{-\zeta_l(\eta)\eta}{J_K(\xi,\eta)}\mathrm{d}\eta\right)_{i,j=1}^{4},\quad l=1,2,3,$$
$$A_3^l(\eta)=\left(\phi_j(\eta)\int_{\hat{I}_i}\frac{-\zeta_l(\xi)(1-\xi)}{J_K(\xi,\eta)}\mathrm{d}\xi\right)_{i,j=1}^{4},\quad l=1,2,3,\qquad \bar{A}_3^l(\eta)=\left(\phi_j(\eta)\int_{\hat{I}_i}\frac{-\zeta_l(\xi)\xi}{J_K(\xi,\eta)}\mathrm{d}\xi\right)_{i,j=1}^{4},\quad l=1,2,3,$$

be matrix functions, where the integral intervals $\hat{I}_1=[0,e_1]$, $\hat{I}_2=[e_1,e_2]$, $\hat{I}_3=[e_2,e_3]$, $\hat{I}_4=[e_3,1]$. Then the block matrices $\mathcal{A}_1$, $\mathcal{A}_2$, $\mathcal{A}_3$ and $\mathcal{A}_4$ can be written as

$$\mathcal{A}_1=\Big(\big(\zeta_j(e_i)\big|\widetilde{Q_{i0}Q_{i4}}\big|^2\big)A_1(e_i)\Big)_{i,j=1}^{3},\quad \mathcal{A}_4=\Big(\big(\zeta_j(e_i)\big|\widetilde{Q_{0i}Q_{4i}}\big|^2\big)A_4(e_i)\Big)_{i,j=1}^{3},$$
$$\mathcal{A}_2=\Big(\big(\widetilde{P_{11}P_{41}}\cdot\widetilde{Q_{i0}Q_{i4}}\big)A_2^j(e_i)+\big(\widetilde{P_{14}P_{44}}\cdot\widetilde{Q_{i0}Q_{i4}}\big)\bar{A}_2^j(e_i)\Big)_{i,j=1}^{3},$$

and

$$\mathcal{A}_3=\Big(\big(\widetilde{P_{11}P_{14}}\cdot\widetilde{Q_{0i}Q_{4i}}\big)A_3^j(e_i)+\big(\widetilde{P_{41}P_{44}}\cdot\widetilde{Q_{0i}Q_{4i}}\big)\bar{A}_3^j(e_i)\Big)_{i,j=1}^{3}.$$

https://doi.org/10.4208/aamm.2013.m401 Published online by Cambridge University Press

We assume that K is a parallelogram firstly. Let $\theta=\angle P_{4,1}\widetilde{P_{1,1}P_{1,4}}$ be the angle between the vectors $\widetilde{P_{1,1}P_{4,1}}$ and $\widetilde{P_{1,1}P_{1,4}}$, $s=\cos\theta$, and $\kappa=\left|\widetilde{P_{1,1}P_{4,1}}\right|/\left|\widetilde{P_{1,1}P_{1,4}}\right|$. Then denote $\mathcal{A}$ in (3.6) by $\mathcal{B}$, we have

$$\mathcal{B}=\frac{\left|\widetilde{P_{1,1}P_{1,4}}\right|^2}{S_k}\begin{pmatrix}\mathcal{B}_1 & \kappa(s\mathcal{B}_2)\\ \kappa(s\mathcal{B}_2) & \kappa^2\mathcal{B}_1\end{pmatrix},$$

where the block matrices $\mathcal{B}_1=\left(\zeta_j(e_i)B_1\right)_{i,j=1}^3$, $\mathcal{B}_2=\left(B_2^j(e_i)\right)_{i,j=1}^3$, and the matrix $B_1=\left(\int_{\hat{l}_i}\phi_j(\eta)\mathrm{d}\eta\right)_{i,j=1}^4$, the matrix functions

$$B_2^l(\xi)=\left(-\phi_j(\xi)\int_{\hat{l}_i}\zeta_l(\eta)\mathrm{d}\eta\right)_{i,j=1}^4,\quad l=1,2,3.$$

Let $\widetilde{\mathcal{B}}=(\mathcal{B}+\mathcal{B}^T)/2$. Then we have

$$\widetilde{\mathcal{B}}=\frac{\left|\widetilde{P_{1,1}P_{1,4}}\right|^2}{S_k}\begin{pmatrix}\dfrac{\mathcal{B}_1+\mathcal{B}_1^T}{2} & \kappa\dfrac{s(\mathcal{B}_2+\mathcal{B}_2^T)}{2}\\ \kappa\dfrac{s(\mathcal{B}_2+\mathcal{B}_2^T)}{2} & \kappa^2\dfrac{\mathcal{B}_1+\mathcal{B}_1^T}{2}\end{pmatrix}.$$

In view of Lemma 3.2, in order to obtain that the matrix $\widetilde{\mathcal{B}}$ is positive definite, we need only to prove that the matrices $(\mathcal{B}_1+\mathcal{B}_1^T)\pm s(\mathcal{B}_2+\mathcal{B}_2^T)$ are positive definite. Let $\widetilde{\mathcal{B}}_1=\mathcal{B}_1+\mathcal{B}_1^T$ and $\widetilde{\mathcal{B}}_2=\mathcal{B}_2+\mathcal{B}_2^T$. It is easily to verify that the matrix $\widetilde{\mathcal{B}}_1$ is symmetric and positive definite with its minimum eigenvalue $\lambda_{\min}(\widetilde{\mathcal{B}}_1)=0.3396$ which computed by the software Matlab. Then it has the cholesky factorization

$$\widetilde{\mathcal{B}}_1=LL^T,$$

where L is a real lower triangular matrix whose diagonal entries are positive. Then we have

$$\widetilde{\mathcal{B}}_1+s\widetilde{\mathcal{B}}_2=LL^T+s\widetilde{\mathcal{B}}_2=L(I+sL^{-1}\widetilde{\mathcal{B}}_2(L^{-1})^T)L^T. \tag{3.7}$$

Since $L^{-1}\widetilde{\mathcal{B}}_2(L^{-1})^T$ is a real symmetry matrix, it has the factorization

$$L^{-1}\widetilde{\mathcal{B}}_2(L^{-1})^T=Q^T\Lambda Q, \tag{3.8}$$

where $\Lambda=(\lambda_i)$, $i=1,2,\cdots,12$, is a diagonal matrix whose diagonal entries are the eigenvalues of $L^{-1}\widetilde{\mathcal{B}}_2(L^{-1})^T$. Substituting (3.8) into (3.7) yields

$$\widetilde{\mathcal{B}}_1+s\widetilde{\mathcal{B}}_2=LQ^T(I+s\Lambda)QL^T.$$

https://doi.org/10.4208/aamm.2013.m401 Published online by Cambridge University Press

Using the software Matlab, we can compute that the matrix $\widetilde{\mathcal{B}}_1+s\widetilde{\mathcal{B}}_2$ is positive definite for all $-0.9908<s<0.9908$. It is to say, when $|\cos\theta|<0.9908$, $(\mathcal{B}_1+\mathcal{B}_1^T)+s(\mathcal{B}_2+\mathcal{B}_2^T)$ is positive definite. Analogously, we can verify that the matrix $(\mathcal{B}_1+\mathcal{B}_1^T)-s(\mathcal{B}_2+\mathcal{B}_2^T)$ is also positive definite for $-0.9908<s<0.9908$. Now by Lemma 3.2, we know that the matrix

$$\begin{pmatrix} \dfrac{\mathcal{B}_1+\mathcal{B}_1^T}{2} & \kappa\dfrac{s(\mathcal{B}_2+\mathcal{B}_2^T)}{2} \\ \kappa\dfrac{s(\mathcal{B}_2+\mathcal{B}_2^T)}{2} & \kappa^2\dfrac{\mathcal{B}_1+\mathcal{B}_1^T}{2} \end{pmatrix}$$

is positive definite too with its minimum eigenvalue $\lambda_0>0$, which is depending on $\theta=\angle P_{4,1}\widetilde{P_{1,1}P_{1,4}}$. It follows from Regularity assumption KA that

$$\lambda_{\min}(\widetilde{\mathcal{B}})\geq\lambda_0\frac{|\widetilde{P_{1,1}P_{1,4}}|^2}{S_K}\geq C\lambda_0, \tag{3.9}$$

where $\lambda_{\min}(\widetilde{\mathcal{B}})$ is the minimum eigenvalue of $\widetilde{\mathcal{B}}$.

With the above argument, we need only estimate the error between the matrix $\widetilde{\mathcal{A}}=\frac{1}{2}(\mathcal{A}+\mathcal{A}^T)$ on an $h^{1+\tau}$-parallelogram and the matrix $\widetilde{\mathcal{B}}$ on a parallelogram. Let $\mathcal{D}=\widetilde{\mathcal{A}}-\widetilde{\mathcal{B}}$. Under the condition (2.4) and Regularity assumption KA, we can proceed as similarly as Lemma 3.9 in [10] to verify that when h is small enough,

$$|(\mathcal{D})_{ij}|\leq Ch^\tau,\quad 1\leq i,j\leq 24, \tag{3.10}$$

which implies that

$$\lambda_{\max}(\mathcal{D})\leq\|\mathcal{D}\|_\infty\leq Ch^\tau, \tag{3.11}$$

where $\lambda_{\max}(\mathcal{D})$ denotes the maximum eigenvalue of the matrix $\mathcal{D}$ and $\|\cdot\|_\infty$ denotes the infinite norm of a matrix. It follows from the above results that

$$\begin{aligned}\tilde{I}_K(u_h,\Pi_h^*u_h)=&\alpha\frac{\mathcal{A}+\mathcal{A}^T}{2}\alpha^T=\alpha(\widetilde{\mathcal{B}}+D)\alpha^T\\ \geq&\big(\lambda_{\min}(\widetilde{\mathcal{B}})-\lambda_{\max}(\mathcal{D})\big)\alpha\alpha^T\\ =&\big(\lambda_{\min}(\widetilde{\mathcal{B}})-\lambda_{\max}(\mathcal{D})\big)|u_h|^2_{1,h,K}\\ \geq&(C\lambda_0-Ch^\tau)|u_h|^2_{1,h,K}.\end{aligned}$$

Proceeding similarly as Lemma 3.6 in [10] gives

$$|I_K(u_h,\Pi_h^*u_h)-\tilde{I}_K(u_h,\Pi_h^*u_h)|\leq Ch|u_h|^2_{1,h,K}.$$

By virtue of the Poincaré inequality, for sufficiently small h,

$$\begin{aligned}a(u_h,\Pi_h^*u_h)=&\sum_{K\in\mathcal{T}_h}\tilde{I}_K(u_h,\Pi_h^*u_h)+\sum_{K\in\mathcal{T}_h}(I_K(u_h,\Pi_h^*u_h)-\tilde{I}_K(u_h,\Pi_h^*u_h))\\ \geq&(C\lambda_0-Ch^\tau)|u_h|^2_{1,h}-Ch|u_h|^2_1\\ \geq&(C\lambda_0-Ch^\tau)|u_h|^2_1-Ch|u_h|^2_1\\ \geq&C\|u_h\|^2_1.\end{aligned}$$

https://doi.org/10.4208/aamm.2013.m401 Published online by Cambridge University Press

Thus, we get the desired result. □

Remark 3.1. Note that a so-called elementwise stiffness matrix technique is used in the stability analysis. By applying the analysis technique in Zhang and Zou [31] to quadrilateral meshes, we can expect that the the smallest angle condition may be unnecessary, but our work would coincide with that of Zhang and Zou's [34] submitted in 2013. Compared to the technique used in [31], the technique used in this paper is suitable for the general dual partitions case (for instance, we use equidistant points for dual partition).

Using the ellipticity of the bilinear form $a(\cdot,\Pi_h^*\cdot)$, we can prove the following H^1 error estimate.

Theorem 3.1. *Suppose that $u\in H_0^1(\Omega)\cap H^4(\Omega)$, u_h is the solution to the FVEM scheme* (2.7)*. If the conditions* (2.3a), (2.3b) *and* (2.4)*, and Regularity assumption KA hold, then for sufficiently small h, there exists a positive constant C independent of h, such that*

$$\|u-u_h\|_1\leq Ch^3\|u\|_4.$$

Proof. The proof of this Theorem is similar to that of Theorem 3.10 in [10]. □

4 Stability analysis of bilinear finite volume element method

In this section, we apply the so-called elementwise stiffness matrix analysis technique to the stability analysis of bilinear finite volume element method (cf. [21]). For simplicity of presentation, we only introduce the details which are different from the bicubic finite volume element scheme.

Let $\mathcal{T}_h$ be a partition of Ω into convex quadrilaterals as described in Section 2. For any element $K\in\mathcal{T}_h$ with vertices P_i, $i=1,2,3,4$, let M_i denote the midpoint of edge P_iP_{i+1}, $(P_5=P_1)$ and Q denote its average center, as in Fig. 3. Then the control volumes in K of the vertex P_i are the subregions $P_iM_iQM_{i-1}$, $(M_0=M_4)$. For each inner vertex P, the associate control volume K_P^* is the union of the above subregions, sharing the vertex P. The set of all the control volumes forms a dual partition $\mathcal{T}_h^*$.

Denote by $U_h(\widehat{K})$ the standard bilinear polynomial space on $\widehat{K}$, then define the trial function space as

$$U_h=\{u_h\in H_0^1(\Omega):u_h|_K=\widehat{u}_h\circ F_K^{-1},\ \widehat{u}_h\in U_h(\widehat{K}),\ K\in\mathcal{T}_h\}.$$

Define the test function space as

$$V_h=\{v_h\in L^2(\Omega):v_h|_{K_P^*}=\text{constant},\ P\in\dot{\Omega}_h\}.$$

We introduce the following discrete semi-norm $|\cdot|_{1,h}$ for U_h

$$|u_h|_{1,h}=\Big(\sum_{K\in\mathcal{T}_h}|u_h|_{1,h,K}^2\Big)^{\frac{1}{2}},\quad \forall u_h\in U_h,$$

https://doi.org/10.4208/aamm.2013.m401 Published online by Cambridge University Press

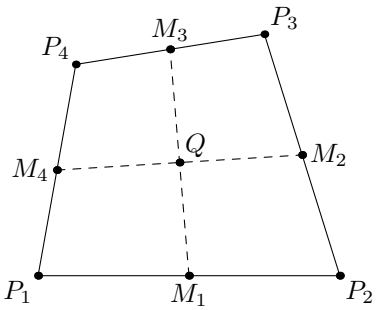


Figure 3: Control volumes in a quadrilateral element for bilinear element.

where

$$|u_h|^2_{1,h,K} = \big(u_h(P_2)-u_h(P_1)\big)^2+\big(u_h(P_3)-u_h(P_4)\big)^2 + \big(u_h(P_4)-u_h(P_1)\big)^2+\big(u_h(P_3)-u_h(P_2)\big)^2.$$

Lemma 4.1. *Suppose that the partition $\mathcal{T}_h$ satisfies the condition* (2.4) *and Regularity assumption KA. Then for sufficiently small h, there exists a positive constant C such that*

$$a(u_h,\Pi_h^* u_h) \geq C\|u_h\|_1^2, \quad u_h \in U_h. \tag{4.1}$$

Proof. Rearranging the terms by element gives

$$\begin{aligned} a(u_h,\Pi_h^* u_h) &= -\sum_{K_P^*\in\mathcal{T}_h^*}\int_{\partial K_P^*}(A\nabla u_h)\cdot\mathbf{n}\Pi_h^* u_h ds \\ &:= \sum_{K\in\mathcal{T}_h} I_K(u_h,\Pi_h^* u_h), \quad \forall u_h \in U_h, \end{aligned} \tag{4.2}$$

with

$$I_K(u_h,\Pi_h^*\bar{u}_h) = \sum_{l=1}^{4}(\bar{u}_h(P_{l+1})-\bar{u}_h(P_l))\int_{\overline{M_lQ}}(A\nabla u_h)\cdot\mathbf{n}ds, \tag{4.3}$$

where $P_5 = P_1$. Define an approximate bilinear form $\tilde{I}_K(\cdot,\cdot)$ on K as follows:

$$\tilde{I}_K(u_h,\Pi_h^*\bar{u}_h) = \sum_{l=1}^{4}(\bar{u}_h(P_{l+1})-\bar{u}_h(P_l))\int_{\overline{M_lQ}}(A(Q)\nabla u_h)\cdot\mathbf{n}ds.$$

Let Z denote the vector related to u_h on K satisfying

$$Z \equiv [u_h(P_2)-u_h(P_1),\ u_h(P_3)-u_h(P_4),\ u_h(P_4)-u_h(P_1),\ u_h(P_3)-u_h(P_2)].$$

Denote by

$$\varphi_1(t) = 1-t, \quad \varphi_2(t) = t,$$

https://doi.org/10.4208/aamm.2013.m401 Published online by Cambridge University Press

the linear polynominal basis in one dimension, then

$$\tilde{I}_K(u_h,\Pi_h^*\bar{u}_h)=Z\mathcal{A}Z^T=Z\frac{\mathcal{A}+\mathcal{A}^T}{2}Z^T, \tag{4.4}$$

where the partition matrix

$$\mathcal{A}=\begin{pmatrix}\mathcal{A}_1 & \mathcal{A}_2\\ \mathcal{A}_3 & \mathcal{A}_4\end{pmatrix}.$$

The entries of these matrices are specified as follows.

$$\begin{aligned}
(\mathcal{A}_1)_{ij}&=|\widetilde{M_1M_3}|^2\int_{\check{I}_i}\frac{\varphi_j(\eta)}{J_K(1/2,\eta)}d\eta, \quad 1\le i,j\le 2,\\
(\mathcal{A}_2)_{ij}&=-\frac{1}{2}\widetilde{P_1P_2}\cdot\widetilde{M_1M_3}\int_{\check{I}_i}\frac{1-\eta}{J_K(1/2,\eta)}d\eta-\frac{1}{2}\widetilde{P_4P_3}\cdot\widetilde{M_1M_3}\int_{\check{I}_i}\frac{\eta}{J_K(1/2,\eta)}d\eta, \quad 1\le i,j\le 2,\\
(\mathcal{A}_3)_{ij}&=-\frac{1}{2}\widetilde{P_1P_4}\cdot\widetilde{M_4M_2}\int_{\check{I}_i}\frac{1-\xi}{J_K(\xi,1/2)}d\xi-\frac{1}{2}\widetilde{P_2P_3}\cdot\widetilde{M_4M_2}\int_{\check{I}_i}\frac{\xi}{J_K(\xi,1/2)}d\xi, \quad 1\le i,j\le 2,\\
(\mathcal{A}_4)_{ij}&=|\widetilde{M_4M_2}|^2\int_{\check{I}_i}\frac{\varphi_j(\xi)}{J_K(\xi,1/2)}d\xi, \quad 1\le i,j\le 2,
\end{aligned}$$

where the integral intervals $\check{I}_1=[0,1/2]$, $\check{I}_2=[1/2,1]$. We assume that K is a parallelogram. Let $\theta=\angle\widetilde{P_2P_1P_4}$ be the angle between the vectors $\widetilde{P_1P_2}$ and $\widetilde{P_1P_4}$, $s=\cos\theta$, and $\kappa=|\widetilde{P_1P_2}|/|\widetilde{P_1P_4}|$. Then denote $\mathcal{A}$ in (4.4) by $\mathcal{B}$, we have

$$\mathcal{B}=\frac{|\widetilde{P_{1,1}P_{1,4}}|^2}{S_k}\begin{pmatrix}\mathcal{B}_1 & \kappa(s\mathcal{B}_2)\\ \kappa(s\mathcal{B}_2) & \kappa^2\mathcal{B}_1\end{pmatrix}.$$

Directly calculating shows

$$\mathcal{B}_1=\begin{pmatrix}3/8 & 1/8\\ 1/8 & 3/8\end{pmatrix}, \quad \mathcal{B}_2=\begin{pmatrix}-1/4 & -1/4\\ -1/4 & -1/4\end{pmatrix},$$

In view of Lemma 3.2, in order to obtain that the matrix $\mathcal{B}$ is positive definite, we need only to prove that the matrices $\mathcal{B}_1\pm s\mathcal{B}_2$ are positive definite.We can proceed as similarly as Lemma 3.3 in Section 3 to verify that $\mathcal{B}_1\pm s\mathcal{B}_2$ are positive definite for all $-1<s<1$. Since the rest of the proof is the same as Lemma 3.3, we omit the details of the proof. □

5 Numerical experiments

In this section, we shall present some numerical examples to check the theoretical results developed in the third section.

https://doi.org/10.4208/aamm.2013.m401 Published online by Cambridge University Press

Example 5.1. Let $\Omega:=(0,1)\times(0,1)$ and consider the following second order elliptic boundary value problem:

$$-\nabla\cdot(A(x,y)\nabla u)=f \qquad \text{in } \Omega, \tag{5.1a}$$

$$u=0 \qquad \text{on } \partial\Omega, \tag{5.1b}$$

where

$$A(x,y)=\begin{pmatrix} e^{2x}+y^2+1 & e^{x+y} \\ e^{x+y} & e^{2y}+x^2+1 \end{pmatrix}.$$

We choose $u=100\sin(7\pi x)(1-x)^3y^5(1-y)^7$ as the exact solution. The source term $f(x,y)$ is determined by the above data.

Two kinds of initial quadrilateral meshes are used in our experiments. The first kind of initial coarse meshes is trapezoidal meshes which are gotten by moving some inner vertices of square meshes by $\pm 0.5h$ along longitudinal direction (see Fig. 4), and the second is random meshes which are obtained by perturbing randomly inner vertices of square meshes within $0.2h$ (see Fig. 5). The numbers of elements of initial coarse meshes are all $4\times 4=16$, and the refined partitions are obtained by symmetric refinement of quadrilaterals via bisection on edges, then condition (2.4) is satisfied.

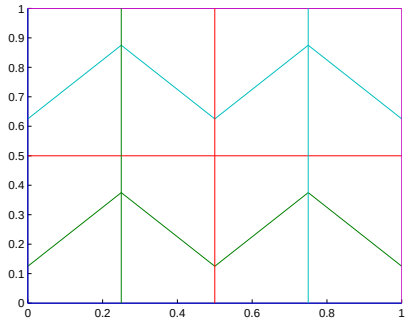


Figure 4: Trapezoidal mesh for Example 5.1.

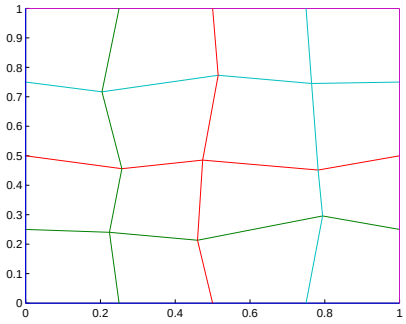


Figure 5: Random mesh for Example 5.1.

As shown in Fig. 6, the bicubic finite volume method has optimal $\mathcal{O}(h^3)$ convergence rate in H^1 norm and $\mathcal{O}(h^4)$ convergence rate in L^2 norm. We also obtain the $\mathcal{O}(h^4)$ superconvergence of the average gradient of numerical solution with our new scheme at the optimal stress points for bicubic interpolation in all elements. The error of average gradient is given by

$$\text{Error}=\Big(\frac{1}{r}\sum_{P\in M}|\overline{\nabla}(u-u_h)(P)|^2\Big)^{1/2},$$

where M is the set of optimal stress points for bicubic interpolation. $\overline{\nabla}$ denotes the average value of gradient ∇ in elements which P belongs to, and r is the number of points in M. The L^2 error estimate and the superconvergence of the average gradient need further research.

https://doi.org/10.4208/aamm.2013.m401 Published online by Cambridge University Press

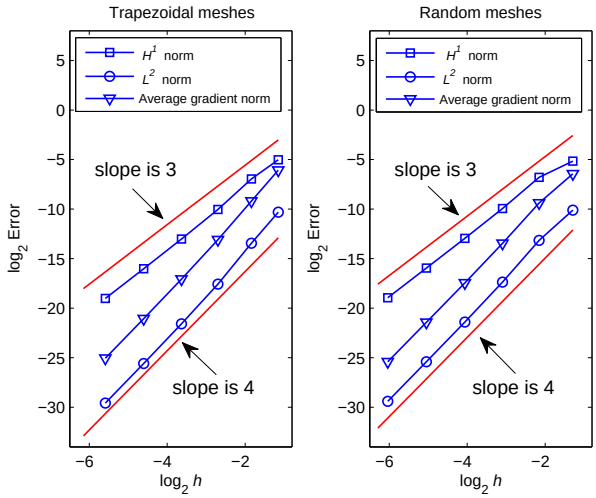


Figure 6: The numerical results of Example 5.1.

Example 5.2. In this example, we consider the same second order elliptic boundary value problem with Example 5.1. In particular, we take the Eq. (5.1a) on parallelogram domain Ω (see Fig. 7). Here, the sides parallel to x axis and the height parallel to y axis are 1 in length, and the minimum angle is 6°. The source term $f(x,y)$ is chosen such that

$$u=100\sin\left(7\pi\left(x-\frac{1}{\tan 6^\circ}y\right)\right)\left(1-x+\frac{1}{\tan 6^\circ}y\right)^3 y^5(1-y)^7.$$

is the exact solution of problem (5.1a) and (5.1b).

The initial parallelogram mesh is shown in Fig. 8. The number of elements is $4\times 4=16$, and the refined partitions are obtained by symmetric refinement of parallelogram via bisection on edges. Then, the minimum angle of each element in the primal partitions is 6 degree.

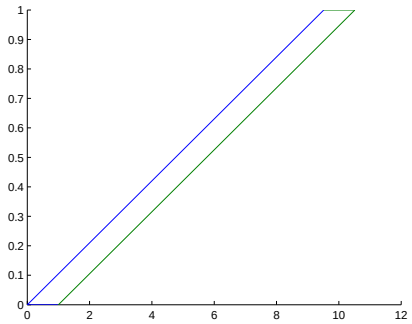


Figure 7: The computational domain for Example 5.2.

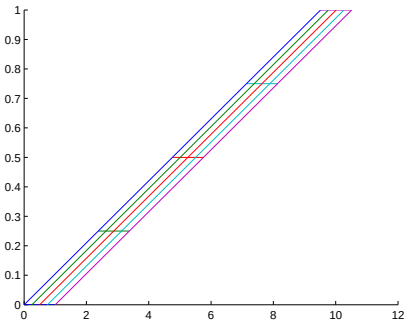


Figure 8: Initial mesh for Example 5.2.

https://doi.org/10.4208/aamm.2013.m401 Published online by Cambridge University Press

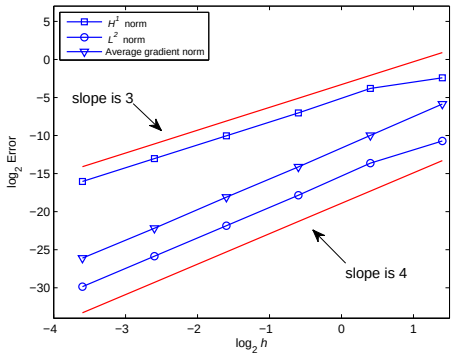


Figure 9: The numerical results of Example 5.2

Shown in Fig. 9 are the numerical results of Example 5.2. We observe that the bicubic finite volume method still has optimal $\mathcal{O}(h^3)$ convergence rate in H^1 norm, $\mathcal{O}(h^4)$ convergence rate in L^2 norm and $\mathcal{O}(h^4)$ superconvergence of the average gradient, which means that the minimal angle (7.7779°) condition is sufficient but not necessary condition for the stability analysis. We conclude that the technique used in stability analysis can be improved.

Acknowledgments

The authors are supported by the 985 program of Jilin University, the National Natural Science Foundation of China (NO. 11371170).

References

[1] Z. Cai, *On the finite volume element method,* Numer. Math., 58(7) (1991), pp. 713–735.
[2] Z. Cai, J. Mandel and S. McCormick, *The finite volume element method for diffusion equations on general triangulations,* SIAM J. Numer. Anal., 28 (1991), pp. 392–402.
[3] J. Huang and S. Xi, *On the finite volume element method for general self-adjoint elliptic problems,* SIAM J. Numer. Anal., 35(5) (1998), pp. 1762–1774.
[4] S. H. Chou, D. Y. Kwak and Q. Li, *L^p error estimates and superconvergence for covolume or finite volume element methods,* Numerical Methods Partial Differential Equations, 19(4) (2003), pp. 463–486.
[5] H. Wu and R. Li, *Eerror estimate for finite volume element methods for general second order elliptic problem*, Numerical Methods for Partial Differential Equations, 19 (2003), pp. 693–708.
[6] P. Chatzipantelidis, *A finite volume method based on the Crouzeix-Raviart element for elliptic PDE's in two dimensions,* Numer. Math., 82 (1999), pp. 409–432.
[7] E. Süli, *Convergence of finite volume schemes for Poissons equation on nonuniform meshes,* SIAM J. Numer. Anal., 28 (1991), pp. 1419–1430.
[8] S. H. Chou and X. Ye, *Unified analysis of finite volume methods for second order elliptic problems,* SIAM J. Numer. Anal., 45 (2007), pp. 1639–1653.

https://doi.org/10.4208/aamm.2013.m401 Published online by Cambridge University Press

[9] S. H. CHOU, D. Y. KWAK, AND K. Y. KIM, *A general framwork for constructing and analyzing mixed finite volume methods on quadrilateral grids: the overlapping covolume case,* SIAM J. Numer. Anal., 39 (2001), pp. 1170–1196.
[10] M. YANG, *A second-order finite volume element method on quadrilateral meshes for elliptic equations,* M2AN, 40 (2006), pp. 1053–1067.
[11] T. WANG AND Y. GU, *Superconvergent biquadratic finite volume element method for two-dimensional Poissons equations,* J. Comput. Appl. Math., 234(2) (2010), pp. 447–460.
[12] J. LV AND Y. LI, *Optimal biquadratic finite volume element methods on quadrilateral meshes,* SIAM J. Numer. Anal., 50(5) (2012), pp. 2379–2399.
[13] Z. CHEN, R. LI, AND A. ZHOU, *A note on the optimal L^2-estimate of the finite volume element method,* Adv. Comput. Math., 16 (2002), pp. 291–303.
[14] F. LIEBAU, *The Finite volume element method with quadratic basis functions,* Computing, 57 (1996), pp. 281–299.
[15] M. YANG, J. LIU AND C. CHEN, *Error estimation of a quadratic finite volume method on right quadrangular prism grids,* J. Comput. Appl. Math., 229 (2009), pp. 274–282.
[16] W. CAO, Z. ZHANG AND Q. ZOU, *Superconvergence of any order finite volume schemes for 1D general elliptic equations,* J. Sci. Comput., 56 (2013), pp. 1–25.
[17] Z. CHEN, *L^2 estimates of linear element generalized difference schemes,* Acta Sci. Natur. Univ. Sunyaseni, 4 (1994), pp. 22–28.
[18] Z. CHEN, *Superconvergence of generalized difference methods for elliptic boundary value problem,* Numer. Math. J. Chinese Univ. (English Ser.), 3 (1994), pp. 163–171.
[19] Z. CHEN, *The error estimate of generalized difference methods of 3rd-order Hermite type for elliptic partial differential equations,* Northeast. Math., J., 8 (1992), pp. 127–135.
[20] R. LI, Z. CHEN AND W. WU, Generalized Difference Methods for Differential Equations, Marcel Dekker, New York, 2000.
[21] Y. LI AND R. LI, *Generalized difference methods on arbitrary quadrilateral networks,* J. Comput. Math., 17(6) (1999), pp. 653–672.
[22] W. WU AND R. LI, *A generalized difference method for solving one-dimensional second-order elliptic and parabolic differential equations,* Chinese Ann. Math. Ser. A, 5(3) (1984), pp. 303-312 (in Chinese).
[23] P. ZHU AND R. LI, *Generalized difference methods for second order elliptic partial differential equations (II)-quadrilateral grids,* Numer. Math. J. Chinese Univ., 4 (1982), pp. 360–375.
[24] M. TIAN AND Z. CHEN, *Quadratic element generalized difference methods for elliptic equations,* Numer. Math. J. Chinese Univ., 2 (1991), pp. 99–113.
[25] R. E. BANK AND D. J. ROSE, *Some error estimates for the box method,* SIAM J. Numer. Anal., 24(4) (1987), pp. 777–787.
[26] W. HACKBUSCH, *On first and second order box schemes,* Computing, 41 (1989), pp. 277–296.
[27] T. SCHMIDT, *Box schemes on quadrilateral meshes,* Compting, 51 (1993), pp. 271–292.
[28] S. H. CHOU AND Q. LI, *Error estimates in L^2, H^1 and L^∞ in covolume methods for elliptic and parabolic problems: a unified approach,* Math. Comput., 69(229) (2000), pp. 103–120.
[29] R. E. EWING, M. LIU, AND J. WANG, *Superconvergence of mixed finite element aproximations over quadrialterals,* SIAM J. Numer. Anal., 36 (1999), pp. 772–787.
[30] Z. CHEN, J. WU AND Y. XU, *Higher-order finite volume methods for elliptic boundary value problems*, Adv. Comput. Math., 37(2) (2012), pp. 191–253.
[31] Z. ZHANG AND Q. ZOU, *A family of finite volume schemes of arbitrary order on rectangular meshes,* J. Sci. Comput., 58 (2014), pp. 308–330.
[32] Z. SHI, *A convergence condition for the quadrilateral wilson element,* Numer. Math., 44 (1984),

https://doi.org/10.4208/aamm.2013.m401 Published online by Cambridge University Press

pp. 349–361.
[33] P. G. CIARLET, The Finite Element Methods for Elliptic Problems, North-Holland, Amsterdam, 1978.
[34] Z. ZHANG AND Q. ZOU, *Finite volume schemes of any order over quadrilateral meshes,* Numer. Math., DOI 10.1007/s00211-014-0664-7, 2014.
[35] J. XU AND Q. ZOU, *Analysis of linear and quadratic simplitical finite volume methods for elliptic equations,* Numer. Math., 111 (2009), pp. 469–492.

https://doi.org/10.4208/aamm.2013.m401 Published online by Cambridge University Press